Wind Gustiness and Proper Air Density Effects on Wave Modelling

Luigi Cavaleri

Istituto Studio Dinamica Grandi Masse, Venice, Italy.

Saleh Abdalla and Peter Janssen

European Centre for Medium-Range Weather Forecasts, Reading, UK.

The characteristics of wind variability are briefly reviewed from wave modelling point of view. Various approaches to represent wind gustiness, to estimate the amplitude of its variability and to introduce its impact to wave models are outlined. The impact of gustiness on the evolution of wave fields is investigated using stand-alone wave model tests. The introduction of gustiness leads to an evident average increase of the resulting wave heights in the open ocean (the Atlantic). This impact is rather limited in enclosed basins (the Mediterranean). The impact of the use of properly evaluated variable air density is also explored. This leads to an increase of the wave heights in the Atlantic especially under cold wind flow in the northern parts. Such impact is very limited in the Mediterranean. Wind gustiness and variable air density were implemented at ECMWF since 9 April 2002. Tests using high resolution model suggested general positive impact.

1. INTRODUCTION

The results of wind-wave prediction have experienced a rather high degree of improvements during the last few years. The current global bias in predicted significant wave height compared to ERS-2 satellite radar altimeter (RA) observation is only few centimetres for the operational model at European Centre for Medium-Range Weather Forecasts (ECMWF, Reading, U.K.). On the other hand, the global root mean square difference (RMSE) was slightly higher than 30 cm in the first three months of 2002 [*Abdalla et al.*, 2002]. Although this is quite an achievement compared to the RMSE of more than 40 cm about 4 years ago, this value may still be considered a high value for some practical applications. Apart from the wave model enhancements over the last few years, part of the improvement in the wave predictions can be associated to the improvements in the driving wind fields. The wind speed global bias is as small as few cm/s, while its RMSE is around 1.4 m/s. This explains the similar error behaviour in the significant wave height.

The continuous improvements to the physics, numerics, resolution and data assimilation schemes together with the larger amount of assimilated observations, especially the satellite observations, are among the factors to be acknowledged for the relatively low errors. The slower rate of reduction in the RMSE values is an indication that, although the current atmospheric models seem to be able to solve for the mean atmospheric properties successfully, they fail to resolve the rather small-scale variability [see *Simmons*, 1991; *Cavaleri et al.*, 1997]. Of course the consequences are felt also in all the applications, including wave modelling, using as input the wind fields.

The variability of the atmosphere is present basically at all the scales, from micro-turbulence, passing through the synoptic level, duly represented in the meteorological models, and above. This paper attempts to provide some guidelines to estimate the implications of these oscillations, which we will refer to as gustiness, for the evaluation of wind waves in the oceans.

There have been few attempts to introduce the impact of gustiness into wave models for practical uses. *Cavaleri and Burgers* [1992] used sequences of random numbers, normalised in amplitude and correlated in time, to simulate the time series recorded at open sea stations. This technique, once applied to real storms [*Komen et al.*, 1994, pp. 326-329], led to an improvement of the model results. However, the level of gustiness was not objectively determined, and taken as constant in space and time. *Ponce and Ocampo-Torres* [1998] explored the sensitivity of a wave model to wind variability. In particular they used an extended series of high frequency wind measurements in the

Gulf of California to estimate the variability to be added to the output fields of a meteorological model. They found an induced increase of the resulting wave heights and a broadening of the directional spectra.

Bauer and Weisse [2000] followed a rather sophisticated approach, using EOF to derive a numerical representation of gustiness from a long-term record of wind speed in the open sea. They were quite successful in reproducing the gustiness spectrum, and went on applying it to a winter hindcast in the North Atlantic Ocean. The results indicated a mild, but clear, increase of the significant wave heights. However, the significance of their results is somehow limited by the use of a gustiness that was numerically sophisticated, but uniform in space and time. As a matter of fact the level of gustiness can change dramatically, depending on the characteristics of the atmosphere and the ocean [see for example *Komen et al.*, 1994, p. 271].

Abdalla and Cavaleri [2002] provided a semi-empirical approach, supported by experimental evidence, for modelling and quantifying the gustiness. The approach implements the Monte-Carlo simulation technique. They used that approach to investigate the implications of gustiness on wave growth and provided comparison with measurements. The approach followed by *Abdalla and Cavaleri* [2002] is not suitable for operational wave models, where the interest is focused on the mean impact rather than on an individual realisation. *Abdalla* [2001] presented a more appropriate approach for operational systems.

The main aim of this paper is to sum up the recent developments and to provide some guidelines to estimate the implications of gustiness for wave modelling to be used in practical applications. In so doing, we will implicitly assume, as all the quoted previous attempts, that the wind is constant during each integration time step of the model. The implications of neglecting the higher frequency wind oscillations will be discussed as well.

Besides wind speed, the momentum (and energy) transfer from air to sea depends also on the air density. This dependence is included in wave models via the wind input source term. However, the wave models usually assume a constant air density ($\rho_a \approx 1.225$ kg/m^3) throughout. The implications of the use of the estimated *correct* value of the air density in the wave model are presented.

2. WIND INPUT SOURCE TERM

The WAM wave model [*WAMDI Group*, 1988; *Komen et al.*, 1994] integrates, numerically, the wave action balance equation using an explicit scheme (first order upwind scheme) for the advection terms and a semi-implicit scheme for the source function terms. The source function consists of terms accounting for wind input [*Miles*, 1957; *Janssen*, 1991], nonlinear wave-wave interaction [*Hasselmann*, 1962; *Hasselmann et al.*, 1985] and the wave dissipation due to white capping [*Hasselmann*, 1974; *Komen et al.*, 1984; *Janssen et al.*, 1989] in addition to other terms to account for processes in finite water depths, when applicable. Detailed description of the model is provided by *Komen et al.* [1994]. Wind gustiness and air density affect wave growth through the wind input source term, which is our focal point of attention.

Miles [1957] proposed a theoretical expression to estimate the rate of energy transfer from a steady and uniform wind to waves in the form:

$$\frac{\partial F}{\partial t} = \gamma \, F \tag{1}$$

Here F is the spectral energy of the wave component, t is time and γ is the wave energy growth rate which has a functional form similar to [see, e.g., *Snyder et al.*, 1981]:

$$\gamma = \gamma \left(\rho_a / \rho_w \;,\; U \cos\phi - c \right) \tag{2}$$

where ρ_a and ρ_w are the air and the water densities, respectively, U is a generic wind speed (which may be replaced by its equivalent in terms of 10-meter wind speed, U_{10}, or wind friction velocity, u_*, as is the case in WAM model Cycle 4), ϕ is the angle between wind and wave propagation directions, and c is the wave phase velocity. Several researchers such as *Snyder et al.* [1981], *Komen et al.* [1984] and *Janssen* [1991] proposed modified growth expressions to replace the one originally proposed by *Miles* [1957], which was found to result in much lower growth rates than suggested by the measurements. The present version of WAM model (Cycle 4) uses the expression proposed by *Janssen* [1991].

In general, all theoretical and experimental works lead to the result that the energy transfer from wind to waves occurs when the wind (component) moves faster than the waves, $U\cos\phi - c > 0$. For wind slower than the phase speed of the waves, $U\cos\phi - c < 0$, there is no energy transfer from wind to waves.

3. WIND GUSTINESS AND ITS IMPACT ON WAVE GROWTH

3.1. Characteristics of Wind Gustiness

There is a fair amount of information on the variability of the atmosphere at the different scales. For the purpose of the present study, we can classify the wind variability according to its scale into three main classes:

1. Low-frequency variability with time scales equal to or larger than synoptic scales (several hours). This group is usually fully resolved by meteorological models and presented for wave models without any loss of information.
2. High-frequency variability with time scales lower than synoptic scales but much larger than typical wind-wave periods (few minutes to few hours). This group is partly resolved in the atmospheric models but lost when the winds are archived, typically at three- or six-hour intervals. This type of variability is the topic of our study and which we term as “wind gustiness”.
3. Sub-grid variability with time scales in the order of the typical wind-wave periods (seconds). This group is not resolved by atmospheric models. It should be stressed that the approaches presented hereafter are not suitable for this kind of variability. Modifications to the theory of wind input need to be introduced in a manner similar to the approach followed by *Miles and Ierley* [1998].

Based on satellite data, *Freilich and Chelton* [1986] and *Tournadre and Blanquet* [1994] provided a general description of the characteristics of surface winds on the oceans. However, their analyses are limited to scales of 200 and 20 km, respectively. Smaller scale variability is usually explored in time using *in-situ* wind measurements. Several dedicated experiments were conducted to study the small-scale characteristics, e.g. Humidity Exchange over the Sea (HEXOS) programme [*Smith et al.*, 1990]. Notwithstanding this wealth of information on wind gustiness, most of it has not yet found its way to wave modelling. There are several reasons behind this:

1. Apart from coupled atmospheric-wave models (and special case studies), the information available from the meteorological models is available only at the archiving interval. This puts an immediate lower limit on the scales of wind variability one can objectively have at disposal.
2. Most meteorological models introduce for numerical stability reasons some numerical diffusion in the lower layers, which tends to further smear the finest details of the field [see *Simmons*, 1991; *Cavaleri et al.*, 1997]. So even in the case of coupled atmospheric-wave models or dedicated special case studies, variability at scales lower than several model integration steps are smoothed out as a result.
3. Finally, the theory itself can not explain the large level of gustiness found under certain conditions in the measured data [see, e.g.; *Panofsky and Dutton*, 1984].

We want to stress that, apart from the practicalities of operational applications, high resolution modelling in space and time is not necessarily a solution, as part of the above limitations still hold.

For our present interests it seems therefore that the level of wind variability present in the atmosphere is partially filtered in the available meteorological model data. The level of filtering depends on the wavelength, increasing towards its lower values, and, for the wave hindcast purposes, with a drastic cut off established by the frequency of archiving.

One way to overcome the above limitations for wave modelling is to superimpose to the input wind fields some numerical variability with characteristics consistent with the available theoretical and experimental information and the specific conditions at the spot, in space and time, under consideration. Our first task is the determination of a suitable algorithm for the numerical representation of gustiness.

General information on the spectra of surface winds is well documented in the literature. *Freilich and Chelton* [1986] analysed scatterometer data in the northern and the southern hemispheres and found the wave number dependence of the kinetic energy spectrum to be $k^{-2.2}$ and $k^{-1.9}$, respectively. *Tournadre and Blanquet* [1994] analysed both spatial (satellite altimeter) and temporal (platform anemometers) data, and found the spectral slope, in wave number and frequency space, to be similarly close to -1.8. We have analysed extensive records from several stations in the North Atlantic, and found the slope to be -1.7 on the average as can be seen in Figure 1.

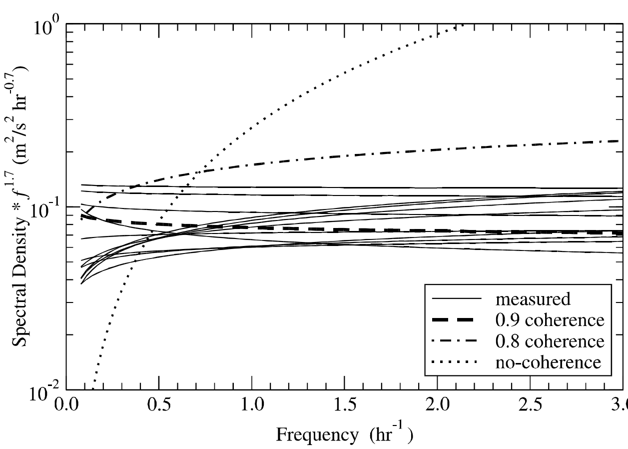

Figure 1. Frequency spectra of wind speed measured at 12 buoys in the Northwest Atlantic together with numerical simulations using Gaussian random numbers with three different levels of coherence (α = 0.9, 0.8 and 0.0). Vertical scale has been normalised by frequency to the power 1.7.

The superposition of a simple Gaussian noise to the model wind data would produce an unrealistic rather white spectrum. One way to avoid this is to introduce a correlation between the sequential data at a given location. This barely reflects the physical evidence that sequential speed values are not independent, but tend to hover around a gradually varying mean. Therefore, following *Cavaleri and Burgers* [1992], for the purpose of this study the wind speed fluctuations were simulated according to:

$$b_i = \alpha\, b_i\text{-}1 + a_i \qquad (3)$$

where b is the sought sequence, a is a sequence of random numbers with a Gaussian distribution of zero mean and unity variance, α is the coherence coefficient with values between 0 and 1, and the subscript denotes rank in the sequence. Expression (3) represents an auto-regressive process of first order, and, with the proper choice of α, leads to realistic time sequences whose spectral characteristics are consistent with the real wind spectra, as discussed above. We have analysed the wind records at our disposal (mainly North Atlantic records) and found on average $\alpha = 0.9$. The sequences produced using this value in (2), has spectral shape in good agreement with the real ones. Minor modifications of α, e.g. $\pm$ 0.05, would cause significant deviations from the realistic spectra. The standard deviation of the constructed sequence σ_b is related to the standard deviation of the random sequence σ_a by [*Box and Jenkins*, 1970]:

$$\sigma_a^2 = (1 - \alpha^2)\, \sigma_b^2 \qquad (4)$$

We are still left with the determination of the value of σ (defined hereafter as the normalised standard deviation by the mean value = $\sigma_{10} / \langle U_{10}\rangle$) under given conditions using the data available in practical applications. According to present theory [e.g. *Panofsky and Dutton*, 1984], σ can reach values close to 10%. However, much larger values of gustiness are possible in nature, as reported by, e.g., *Monahan and Armendariz* [1971] and *Sethuraman* [1979]. The North-Atlantic wind records we analysed, indicated the existence of σ values in excess of 30%. Similar values were derived also from the records obtained from the oceanographic tower of the Istituto Studio Dinamica Grandi Masse, ISDGM [*Cavaleri*, 2000].

Given that the theory does not seem to indicate levels of gustiness as high as suggested by the measurements, for test purposes we look for a more pragmatic approach. One possibility is to correlate the level of gustiness to the local air-sea temperature difference ΔT. We have made use of the data available from the ISDGM oceanographic tower. Within the scatter of the data, the best-fit line suggests the following expression with good approximation:

$$\sigma = \max[0.,0.025\ (T_{water} - T_{air})] \qquad (5)$$

with T_{water} and T_{air} being the water and air temperatures, measured respectively at -5 m and 21 m with respect to the mean sea level.

Although (5) provides a convenient way to quantify wind variability under unstable conditions, it is clear that ΔT may not be enough to account for the instability. A more comprehensive empirical expression to estimate the standard deviation of wind speed is the formula proposed by *Panofsky et al.* [1977] which can be written as:

$$\frac{\sigma_{10}}{\langle u_* \rangle} = \left[b + 0.5 \left(\frac{z_i}{-L} \right) \right]^{1/3} \qquad (6)$$

where $\langle u_* \rangle$ is the mean wind friction velocity, z_i is the height of the lowest inversion, L is the Monin-Obukhov length, and b is a constant representing the background gustiness level that exists all the times, irrespective of the stability conditions. The impact of the background level of gustiness is already included implicitly in the parameterisations of the atmospheric model as well as in the wave model. Therefore for practical applications, the constant b value in (6) is taken as 0. The quantity $(z_i / -L)$, which is a measure for the atmospheric stability, is usually computed during the integration procedure, making it available for wave models coupled with atmospheric models. This is not the case for stand-alone wave models, causing (5) to be an attractive alternative for (6).

Coherence in time, as expressed by (3), implies also coherence in space. The general view of gustiness superimposed to a uniform wind field can be compared to a wavy surface, with the single oscillation propagating mainly along the wind direction. The practical problem is the quantification of the coherence in space. *Tournadre and Blanquet* [1994] provide estimates of spectra down to the scale of 20 km. However, their data have been filtered to eliminate the high frequency oscillations. An estimate can be obtained considering the advection of turbulence by the wind field [*Panofsky and Dutton*, 1984]. Starting from the coherence in time, and assuming a mean wind speed of, e.g., 15 m/s, this suggests a comparable coherence in space at distances of the order of 10 km. The grid resolution of the wave model dictates the significance of the spatial coherence. As better explained later in Section 4, we used resolutions between 0.25 and 1 degree for our tests. While for the lower limit, the coherence between adjacent grid points may still be significant; this is not the case for the upper limit. To carry out all the tests in a consistent manner, we have decided to neglect the spatial coherence, which is consistent with the assumption of *Bauer and Weisse* [2000]. Therefore, the time series derived from (3) are evaluated independently for each grid point.

Besides wind speed, we considered also the oscillations of wind direction. We found that, with the exception of rather low and sparse winds, its fluctuations are rather small and almost independent on the air-sea stability conditions and the level of gustiness of wind speed. For wind speeds larger than 5 m/s, the standard deviation of the wind direction fluctuations was found to have a 4° mean value and a maximum not exceeding 10°. For the simulation, a procedure similar to the one for wind speed was followed.

3.2. Effect on Wave Growth

Three mechanisms lead to an enhancement of the wave field in the presence of gustiness, sorted with the more significant one at the top:

1. As mentioned above, wind is only able to input energy to waves with phase velocity lower than the wind velocity. For a well developed sea, when part of the components in the spectrum have a phase speed larger than the mean wind speed, the excess of energy transferred to the wave spectrum due to an increase of wind speed is not compensated by a corresponding decrease during the opposite phase. This leads to a net positive increase in the energy pumped to the waves in the presence of gustiness compared to a steady wind with the same mean wind speed. Because of the analogy with the filtering capability of an electronic diode, we term this mechanism as *diode* effect.
2. According to various studies [see, e.g., *Smith et al.*, 1990], the variations in the surface wind speed U_{10} are Gaussian distributed. The wave generation mechanism is function of the friction velocity u_*, which is nonlinear (grows faster) with respect to U_{10}. Therefore, the mean u_* is greater than the value of u_* corresponding to the mean U_{10}.
3. According to *Janssen* [1991] formulation, the input to waves has a rather concave dependence on u_*. This enhances slightly the effect of gustiness.

While mechanisms 2 and 3 are active throughout the process, the first one becomes effective only at an advanced stage of development, when energy is present also in the sufficiently low frequency, hence fast, wave components. Therefore, a gusty wind results in marginal enhancement of wave growth at the early stages of development, significant differences being expected only at a later stage.

3.3. Representation of Gustiness in Wave Models

Wind speed as produced by the atmospheric models is assumed as the mean value. Random variations that follow normal distribution with zero mean and variance estimated using either (5) or (6) are therefore superposed on the assumed mean value. There are two approaches to do this:

1. Monte-Carlo simulation approach, where strictly speaking variations are superimposed on model winds using random number generation and the resulting wind is used to force the wave model. This approach provides a kind of instantaneous impact for each realisation. For the mean impact, one needs to carry out several tens of realisations and then evaluate the average of all realisations. This approach is not an efficient one to follow for operational systems where mean impact is usually of interest.
2. Modified input source term approach, where the mean impact of the variations is evaluated analytically beforehand in a form of modified wind input source term. Although this is an attractive method to be used for operational models where several tens of Monte-Carlo realisations is not practical, it does not provide an idea about the magnitude of variability of wave conditions.

3.3.1. Monte-Carlo Approach. For each grid point (5) or (6) can be used to compute the corresponding σ_b value, which leads, through (4), to the corresponding σ_a value. At each wave model integration time step, the $<U_{10}>$ and σ_a fields are evaluated either from the atmospheric model or from interpolated between the bordering synoptic times for stand-alone model runs. The b sequence is constructed using expression (3) and the appropriate α value (0.9). Multiplied by the interpolated σ_a and $<U_{10}>$ values, its superposition to $<U_{10}>$ value itself provides the input wind time series to the wave model.

This procedure provides quasi-realistic sequences of wind speed. Gustiness can be simulated using this approach in three different ways [*Abdalla and Cavaleri*, 2002]:

1. Flip-flop: The variable, a, in (3) is forced to take alternatively the values +1 and –1, and α is set equal to 0. This results in a flip-flop fluctuation that simulates wind gustiness discarding both the randomness and the coherence of the phenomenon.
2. No-coherence: The variable, a, is obtained using a random number generator and follows the Gaussian distribution with zero mean and unity variance. α is set equal to 0. This results in a random fluctuation that simulates wind gustiness discarding its coherence in time.

3. Coherence: The variable, a, is obtained as in the no-coherence case, but $\alpha = 0.9$. This results in a more realistic representation of wind gustiness.

3.3.2. Modified-input source term Approach. The mean impact of gustiness can be evaluated using the following equation, as was first proposed by *Janssen* [1986]:

$$\langle \gamma(u_*) \rangle = \int_{u_*=-\infty}^{\infty} \frac{1}{\sigma_* \sqrt{2\pi}} \exp\left(-\frac{\left(u_* - \langle u_* \rangle\right)^2}{2\,\sigma_*^{\,2}} \right) \gamma(u_*)\, du_* \qquad (7)$$

where u_* represents the instantaneous (unresolved) wind friction velocity, σ_* is the standard deviation of the friction velocity and any quantity embraced by <···> represents the mean value of that quantity over the whole grid-box/time-step. Note that u_* is the (gust-free) value obtained from the atmospheric model. The integral (7) can be approximated using the Gauss-Hermite quadrature:

$$\langle \gamma\,(u_*) \rangle \cong 0.5 \left[\gamma\left(\langle u_* \rangle - \sigma_*\right) + \gamma\left(\langle u_* \rangle + \sigma_*\right) \right] \qquad (8)$$

Expression (8) replaces the classical wind input source term in the wave model. It is quite clear that (8) resembles the flip-flop representation of gustiness described above.

4. NUMERICAL EXPERIMENTS

4.1. Basic Hypothetical Tests

To examine the importance of various impacts and scenarios associated with the wind gustiness, a number of simplified single point runs were carried out. Various mean wind speed values were used. The wind gustiness was simulated using predetermined σ values. The three types of numerical gustiness, namely flip-flop, no-coherence and coherence, were used. Results from all runs are compared against a corresponding reference run which was carried out using steady wind speed. Different wind speeds and levels of gustiness were used in the tests, but only the results obtained with mean wind speed of 15 m/s and $\sigma = 0.25$ are presented here. Apart from the magnitude of the impact, all the other results are consistent with what is reported here.

The significant wave height growth curves of the gusty tests are compared to the reference run in Figure 2. Gustiness has almost no effect on the wave growth during the very early stages. The increase in wave height during the mature and late stages of development is significant, around 1 m or about 20% increase after three days of simulation.

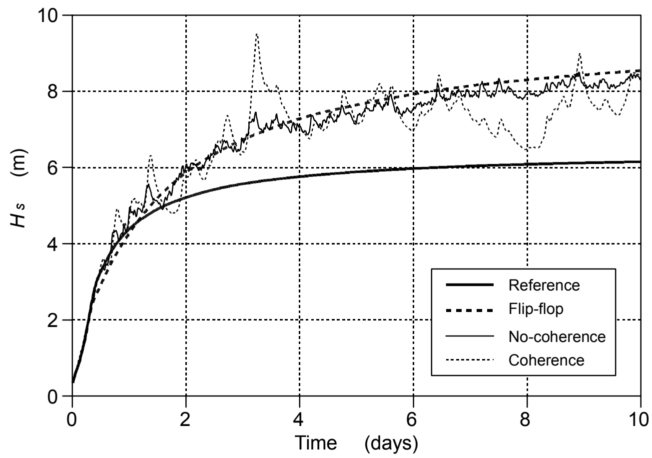

Figure 2. Effect of wind gustiness on the significant wave height growth curves from single point runs with standard integration time step.

The no-coherence growth curve has limited oscillations associated to randomness, and on the average it differs only slightly from the corresponding smooth flip-flop curve. The coherence curve shows large random oscillations of different periods. It is important to realise that these oscillations, introduced in the time series due to the coherence, are significant only from a statistical point of view. Only the average values (in a certain period) and the amplitude of the oscillations can be compared. For a better understanding of their statistical properties, the ensemble technique has been used. The test was repeated 100 times with different random number sequences, and both the average and the envelope of the 100 growth curves are presented in Figure 3, together with the growth curves corresponding to the reference and flip-flop runs. The flip-flop growth curve coincides, more or less, with the mean of the 100 coherence gusty runs.

The implications of wind direction variability on wave modelling were also assessed using several tests in a manner similar to that followed for wind speed. It turned out that introducing random variations of wind direction with standard deviation of 10°, which is the upper limit observed, would lead to a reduction of the significant wave height by about 1% compared to the reference run (not shown). Therefore, it is safe to neglect the effect of the directional variability and to focus only on wind speed variability alone.

Several single-point runs were used to assess the impact of air density variations on wave height compared to the reference run with the standard value of ρ_a of 1.225 kg/m^3. At the very early stages of growth, the wave height differences with respect to the reference run are very small. However, rapid growth of the differences follows afterwards. This is because at this stage the input term is the only one affected by the change of density. The later development shows almost constant H_s differences, when the other processes, e.g. white capping, adapt to the new situation. An increase of 10% in air density results in 5% maximum difference in wave height compared to the reference run. Similar reductions follow for reducing the air density value.

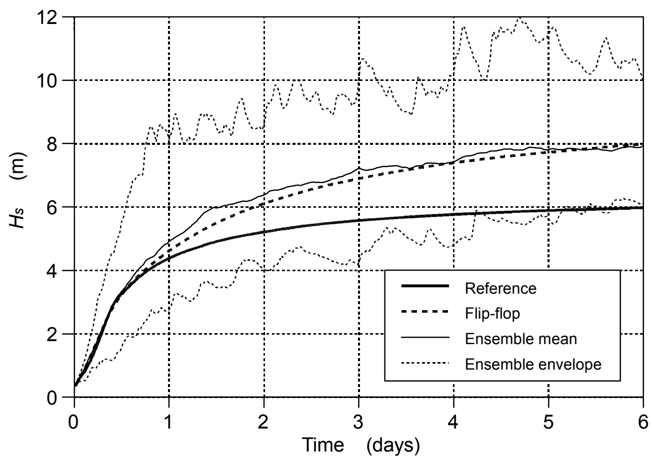

Figure 3. Mean and envelope of the growth curves resulting from 100 coherence runs with different random number sequences. The reference and the flip-flop curves are given for comparison.

4.2. Stand-alone Model Tests

4.2.1. Wind Gustiness Impact. Two long-term hindcast experiments were conducted using stand-alone WAM model. The first was a six-month, winter 1999-2000, hindcast study in the North Atlantic to explore the possible gustiness effects under long fetch conditions in the open ocean. The other experiment was another six-month, winter 1993-1994, continuous wave hindcast study in the Mediterranean Sea to reflect the effect of gustiness under relatively short fetch conditions in rather enclosed basins. Both periods were selected as they are representative for active atmosphere with storms of various types. Monte-Carlo simulation approach was used for those tests with the variability estimated using (5). The wind and temperature data used in the experiments are the analysis surface-wind, U_{10}, air temperature at 2 m height, T_{air}, and sea surface temperature, T_{water}, fields resulted from the ECMWF spectral meteorological model. T319 version, with a spectral resolution of about 60 km, was operational in 1999-2000 while T213 version, with a spectral resolution of about 95 km, was the operational one in 1993-1994 [see *Simmons*, 1991]. Those fields are available every 6 hours, at the major synoptic times. The standard operational WAM model was used with spatial resolution of 1.0° and 0.25°, respectively for the North Atlantic and the Mediterranean, in both longitude and latitude directions.

The most interesting numerical tests are summarised in Table 1. The impact of gustiness is summarised in Table 2. One can conclude that the gustiness impact in the Mediterranean, being an enclosed basin with short fetches, is rather limited. On the other hand the impact in the Atlantic is rather significant. It is important to stress that, with the introduction of gustiness using the Monte-Carlo approach, any comparison can be done only from a statistical point of view. Any realisation of a gusty sequence obtained using this approach is just one of the many possible cases. Even if the physical assumptions underlying the approach are correct, it is most likely that a given time sequence has little to do with what has really happened in nature, except in statistical sense.

It is important to notice that, while the introduction of gustiness and the use of a variable air density are steps in the right direction, it is not expected to be the final solution. The accuracy of the present wave model results is connected to many different factors, physical, numerical, and of course accuracy of the input wind fields. The impact of gustiness and a variable air density varies according to the local conditions. As we will see in the following, this impact is not necessarily larger where we find the largest errors in practical applications. Therefore, while a look at the measurements will certainly be useful, the impact must be judged with respect to a reference non-gusty run, done in the conventional way, without gustiness and with a constant value of the air density.

Table 1. Numerical tests of interest using stand-alone wave model

ID	Forcing	Period	Region
AR	Reference (standard model run)	01 Oct 1999 to 31 Mar 2000	North Atlantic
AN	Gustiness without coherence		
AC	Gustiness with coherence		
AD	Variable air density		
AE	Ensemble (50 members, coherence)	15-20 Dec 99	
MR	Reference (standard model run)	01 Oct 1993 to 31 Mar 1994	Mediterranean
MN	Gustiness without coherence		
MC	Gustiness with coherence		
MD	Variable air density		
ME	Ensemble (50 members, coherence)	21-24 Oct 93	

Table 2. Gustiness and air density impact on predicted significant wave heights for the numerical experiments of Table 1

	AR	AN	AC	AD	MR	MN	MC	MD
Maximum negative difference, m	---	-1.09	-2.35	-0.49	---	-0.75	-1.41	-0.37
Lowest mean, m	4.13	-0.00	+0.00	-0.01	1.44	-0.01	-0.00	-0.01
Highest mean, m		+0.07	+0.20	+0.10		+0.00	+0.03	+0.01
Maximum positive difference, m	14.73	+2.37	+6.59	+1.09	9.57	+0.64	+2.01	+0.33

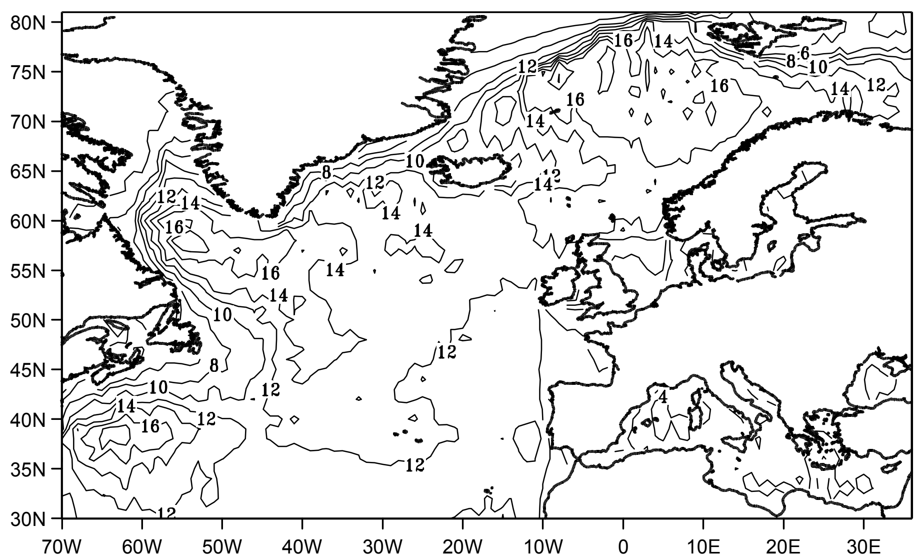

Figure 4. The distribution of the mean differences of significant wave-height, in cm, between the coherence (AC) and the reference (AR) runs in the North Atlantic, during the six-month period.

Figure 4 shows the mean point by point difference of significant wave height between the gusty run AC and the AR run (see Table 1) over the whole period of six months. The differences are limited, but still significant, in between 10 and 15 cm, with local peaks as high as 20 cm. It is interesting to note that these gains in wave height compensate for a major part of the underestimates of the ECMWF wave model, which was operational at the time, compared to the buoy measurements (around 40 cm) as reported by *Bidlot et al.* [2000]. This suggests that the introduction of gustiness can indeed lead to a substantial improvement of the wave results in the North Atlantic.

A detailed comparison of the different hindcasts was done against the wave measured data available at three wave gauging stations: Stations 62026 (55.3°N, 2.3°E) and 62109 (57.0°N, 0.0°E), which are located in the North Sea, and Station 64046 (60.5°N, 5.0°W), which is located in the ocean, north of U.K. These stations were chosen because they are fully (62026 and 62109) or partially (64046) sheltered from the southern swell, not represented in the present tests. At station 64046 the introduction of gustiness leads to a substantial reduction of the six month H_s bias, from -47 to -31 cm, the best results being obtained by the coherence run, AC. The improvement, not so substantial, as expected, because of the randomness introduced in the forcing wind fields, is present also in the RMSE. In the North Sea the results are more neutral, consistently with the already very low bias of the reference H_s. The results from the various *gusty* runs are very similar, with the coherence run having a slight positive bias (a few centimetres) compared to AR and AN runs.

The stormy period between 15 and 20 December 1999 was selected for the ensemble run. This period was characterised by a sustained level of gustiness in the stormy northeastern part of the Atlantic, where wind and wave measurements are available to compare against. During the most active part of the storm, which was 17-19 December, over the Northeastern Atlantic the wind was dominantly northwesterly, with wind speed up to 24 m/s and σ values around 0.2. 50 coherence simulations of the storm, each one with different random number sequences, were carried out. The results of this analysis for station 64046 are given in Figure 5, showing the significant wave heights derived from the measurements, the reference (AR) and the no-coherence (AN) runs in addition to the range (hatched) of the 50 run envelope and their mean. The onset of gustiness is made dramatically evident by the rapid increase of the hatched area in the early hours of 18 December. Note that the gusty runs are almost always higher (larger H_s) than AR. There is a substantial decrease of the average negative bias (62 cm) with respect to the buoy data, down to 47 and 25 cm, for the no-coherence and the ensemble mean, respectively. The flip-flop run (not shown) has results similar to AN.

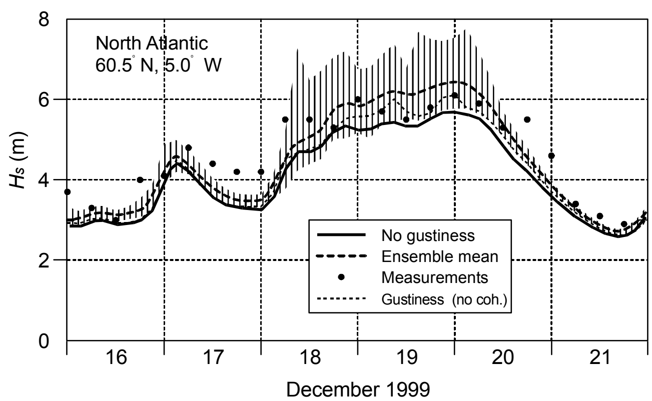

Figure 5. Time histories of significant wave height at buoy 64046 (located at 60.5°N, 5.0°W). Hatched area represents the envelope of the 50 ensemble-runs.

The results from the Mediterranean tests show limited impact of gustiness on the wave height as can be inferred from Table 2. This is due to the fact that the fetch lengths in the Mediterranean are very limited preventing the diode mechanism of gustiness to act at full scale.

4.2.2. Air Density Impact. The impact of using proper air density values in the North Atlantic, AD, compared to the AR run over the whole period of six months can be inferred from Table 2. On average, the air-density variability results in wave height biases not exceeding 10 cm when compared to the reference run. However, instantaneous reductions as large as 50 cm and increases as high as 1.1 m were found. The air density in the North Atlantic is generally higher than the standard value, and varies mostly between 1.1 and 1.5 kg/m^3. This leads to a distributed limited, but always positive, increase of H_s throughout the basin. Looking at the maps of wave height differences between AD and AR runs (not shown), one can find that the average H_s differences throughout the period tend to increase from South to North. The largest average increases occur in the most northerly areas, east of Greenland, and in the Baffin Bay, where there are frequent inflows of cold dense air from the North.

The impact of using the proper air density in the Mediterranean is rather limited as can be seen in Table 2. On average, considering the air density variability leads to wave height variations of less than 1 cm. This is because in general the air density in the Mediterranean does not differ much from the standard value, varying mostly between 1.16 and 1.24 kg/m^3. However, instantaneous H_s differences as high as 37 cm are possible. On the overall basin, most of these values vary between 6 and 8 cm. Expectably, the localised relatively large positive differences are typically associated to northerly flows of cold air, e.g. the Mistral in the northern part of the Western Mediterranean and Bora in the northern part of the Adriatic Sea.

4.3. Coupled Model Tests

For this group of tests, the modified-input source term approach (8) was used together with (6) for the evaluation of the gustiness levels. Most of the experiments with the coupled model used the combined effect of wind gustiness and air density unless otherwise specified. Several experiments were carried out using a low-resolution atmospheric model (T159) coupled with a wave model with 1.5° resolution. The results showed limited positive impact. The more realistic higher resolution T511/L60 model was then used. The spatial resolution of the atmospheric model in T511 is about 40 km while that of the wave model is 55 km. The integration time step is 15 minutes. There is a two-way coupling between the atmospheric and the wave models at each time step. This set-up was run for the period 22 November – 14 December 2000. The general impact of gustiness on the scores of significant wave height compared to the reference run without gustiness for the Northern Hemisphere (NH), Tropics and the Southern Hemisphere (SH) is given in Table 3.

Table 3. General impact of gustiness and air density on significant wave height compared to the reference run for the period 22-29 Nov. 2000.

	Gustiness	Air Density	Both
Northern Hemisphere	Neutral	negative	negative
Tropics	Positive	negative	neutral
Southern Hemisphere	Positive	positive	positive

Comparing the model forecast significant wave heights against the ERS-2 radar altimeter observations shows that the bias in the NH is reduced by 5 cm while the RMSE is almost unchanged when compared to the reference run. For the SH the bias was almost unchanged, but the RMSE was slightly reduced. The impact in the Tropics was almost neutral

Table 4 shows the combined impact of gustiness and air density on the wave height statistics as compared to the wave buoys for the period 22 November – 14 December 2000. Although the impact is minor, it is certainly positive. This should be interpreted keeping in mind that gustiness is limited to specific areas and time periods. Long term averages smoothes out any significant but isolated impact.

Table 4. Impact of gustiness and variable air density on model performance as compared with buoy wave heights for the period 22 Nov. – 14 Dec. 2000 (6805 observations).

	Reference	Gustiness & Air Density
Bias [a], cm	-13.8	-13.3
RMSE, cm	46.9	46.6

[a] Bias = model – buoy, mean buoy H_s = 2.72 m

5. CONCLUSIONS

It is possible to include the impact of wind gustiness on wave growth by either the Monte-Carlo simulation approach or the modified-input source term approach. The former is suitable for providing an envelope and the distribution of the possible impact while the latter provides only the mean impact. There is sufficient evidence to support the use of time coherent random noise to represent wind gustiness. The level of gustiness can be estimated using two different empirical expressions (5) or (6). A more theoretical evaluation would be appreciated, but not expected to change significantly the outcome of the present representation.

The implications of gustiness in the open ocean (the Atlantic) are much larger than those in enclosed basins (the Mediterranean). Wave height increase in the open ocean can be 10-20 cm on average with individual increases in space and time as high as few meters compared to non-gusty runs. In the enclosed basins, the increase is in the order of few centimetres.

The use of proper variable air density in wave models is straightforward. This leads to time-averaged increases of H_s up to 10 cm, with single peak values above one metre in the open ocean. The changes in the Mediterranean are very limited.

The impact of gustiness and the use of quasi-realistic air density were introduced into the coupled atmospheric-wave model of ECMWF. Low resolution model tests indicate positive impact of model results. Tests using the current resolution of T511 for the period 22 November – 14 December 2000 indicated remarkable positive impact in the SH. Although the overall impact in the NH seems to be slightly negative, ERS-2 radar altimeter observations and wave buoy measurements indicates reduction in bias without any significant deterioration in other statistics. The gustiness and air density implementation is operational at ECMWF since 9 April 2002.

REFERENCES

Abdalla, S., Impact of wind gustiness and air density on modelling of wave generation: Implementation at ECMWF, *Proc. ECMWF Workshop on Ocean Wave Forecasting*, 2-4 July 2001, Eur. Cent. For Med. Range Weather Forecasts, Reading, U.K., 147-153, 2001.

Abdalla, S. and L. Cavaleri, Effect of wind variability and variable air density on wave modeling, *J. Geophys. Res.*, in press, 2002.

Abdalla, S., P. Janssen, and J. Bidlot, The use of satellite observations and enhanced physics to improve wind-wave predictions at ECMWF, *Proc. 28th. Intl. Conf. Coastal Eng., ICCE2002*, 7-12 July 2002, Cardiff, Wales, U.K., in press, 2002.

Bauer, E., and R.Weisse, Determination of high-frequency wind variability from observations and application to North Atlantic wave modelling, *J. Geophys. Res., 105*, 26179-26190, 2000.

Bidlot, J., D.J.Holmes, P.A.Wittmann, R.Lalbeharry, and H.S.Chen, Intercomparison of the performance of the operational wave forecasting systems with buoy data, *Tech.Memo. 315*, 46 pp., Eur. Cent. For Med. Range Weather Forecasts, Reading, U.K., 2000.

Box, G.E.P. and G.M.Jenkins, *Time Series Analysis, Forecasting and Control*, 553 pp., Holden Day, S. Francisco, 1970.

Cavaleri, L., The oceanographic tower *Acqua Alta* - activity and prediction of sea states at Venice, *Coastal Eng.*, *39*, 29-70, 2000.

Cavaleri, L. and L. Bertotti, Influence of land on the modelled marine surface wind fields, *ISDGM Report 00-14*, 27pp., Ist. Studio Dyn. Grandi Masse, Venice, Italy, 2000.

Cavaleri, L., L.Bertotti, M.Hortal, and M.Miller, Effect of reduced diffusion on surface wind and wave fields, *Mon. Weather Rev.*, *125*, 3024-3029, 1997.

Cavaleri, L. and G. Burgers, Wind gustiness and wave growth, *KNMI-Preprints*, *92-18*, 38pp., Koninklijk Ned. Meteorol. Inst., De Bilt, The Netherlands, 1992.

Freilich, M.H., and D.B.Chelton, Wavenumber spectra of Pacific winds measured by the Seasat scatterometer, *J. Phys. Oceanogr., 16*, 741-757, 1986.

Hasselmann, K., On the non-linear energy transfer in a gravity-wave spectrum, part 1: general theory, *J. Fluid Mech.*, *12*, 481-500, 1962.

Hasselmann, K., On the spectral dissipation of ocean waves due to white capping, *Boundary Layer Meteorol.*, *6*, 107-127, 1974.

Hasselmann, S., K. Hasselmann, J.H. Allender and T.P. Barnett, Computations and parameterizations of the nonlinear energy transfer in a gravity-wave spectrum, part 2: Parameterization of the nonlinear energy transfer for application in wave models, *J. Physical Oceanogr.*, *15*, 1378-1391, 1985.

Jacob, C., E. Andersson, A. Beljaars, R. Buizza, M. Fisher, E. Gerard, A. Ghelli, P. Janssen, G. Kelly, A.P. McNally, M. Miller, A. Simmons, J. Teixeira, and P. Viterbo, The IFS cycle CY21R4 made operational in October 1999, *ECMWF Newsletter*, *87*, 2-8, 2000.

Janssen, P.A.E.M., On the effect of gustiness on wave growth, *KNMI Afdeling Oceanografisch Onderzoek memo 00-86-18*, 17 pp., Koninklijk Ned. Meteorol. Inst., De Bilt, The Netherlands, 1986.

Janssen, P.A.E.M., Quasi-linear theory of wind generation applied to wave forecasting, *J. Physical Oceanogr.*, *22*, 1600-1604, 1991.

Janssen, P.A.E.M., P. Lionello, M. Reistad and A. Hollingsworth, Hindcasts and data assimilation studies with the WAM model during the Seasat period, *J. Geophys. Res.*, *94*, 973-993, 1989.

Komen, G.J., K. Hasselmann, and S. Hasselmann, On the existence of a fully developed windsea spectrum, *J. Physical Oceanogr.*, *14*, 1271-1285, 1984.

Komen, G.J., L. Cavaleri, M. Donelan, K. Hasselmann, S. Hasselmann and P.A.E.M. Janssen, *Dynamics and Modelling of Ocean Waves*, 532 pp., Cambridge Univ. Press, Cambridge, UK, 1994.

Miles, J.W., On the generation of surface waves by shear flows, *J. Fluid Mech.*, *3*, 185-204, 1957.

Miles, J. and G. Ierley, Surface-wave generation by gusty wind, *J. Fluid Mech.*, *357*, 21-28, 1998.

Monahan, H.H. and P. Armendariz, Gust factor variations with height at atmospheric stability, *J. Geophys. Res.*, *76*, 5807-5818, 1971.

Munn, R.E., *Descriptive Micrometeorology*, 245 pp., Academic Press, New York, 1966.

Panofsky, H.A., and J.A. Dutton, *Atmospheric Turbulence*, 397 pp., John Wiley, New York, 1984.

Ponce, S., and F.J. Ocampo-Torres, Sensitivity of a wave model to wind variability, *J. Geophys. Res.*, *103*, 3179-3201, 1998.

Sethuraman, S., Atmospheric turbulence and storm surge due to Hurricane Belle (1976), *Mon. Weather Rev.*, *107*, 314-321, 1979.

Simmons, A., Development of the operational 31-level T213 version of the ECMWF forecast model, *ECMWF Newsl.*, *56*, 3-13, 1991.

Smith, S.D., K.B. Katzaros, W.A. Oost and P.G. Mestager, Two major experiments in the humidity exchange over the sea (HEXOS) program, *Bull. Am. Meteorol. Soc.*, *71*, 161-172, 1990.

Snyder, R.L., F.W. Dobson, J.A. Elliott and R.B. Long, Array measurements of atmospheric pressure fluctuations above surface gravity waves, *J. Fluid Mech.*, *102*, 1-59, 1981.

Tournadre, J., and S. Blanquet, Wind speed and wave mesoscale variability from *in situ* and altimeter data, *Global Atmos. Ocean Syst.*, *2*, 221-245, 1994.

WAMDI Group, The WAM model–a third generation ocean wave prediction model, *J. Phys. Oceanogr.*, *18*, 1775-1810, 1988.

S. Abdalla, European Centre for Medium-Range Weather Forecasts, Shinfield Park, Reading, Berkshire, RG2 9AX, U.K. (abdalla@ecmwf.int)

L. Cavaleri, Istituto Studio Dinamica Grandi Masse, S. Polo 1364, 30125 Venice, Italy. (L.Cavaleri@isdgm.ve.cnr.it)

P. Janssen, European Centre for Medium-Range Weather Forecasts, Shinfield Park, Reading, Berkshire, RG2 9AX, U.K. (peter.janssen@ecmwf.int)